The SARFID technique for Discriminating Tagged Items Moving Through a UHF-RFID Gate

Alice Buffi and Paolo Nepa

***Abstract*— The discrimination of tagged items moving along a conveyor belt from other tagged items that are present in the scenario is investigated, when a UHF-RFID gate is installed at a conveyor section. Indeed, tagged items that are static or randomly moving in the scenario (nomad tags) around the reader antenna could be detected even if they are not on the conveyor (false positive readings). The classification procedure here proposed exploits the SARFID phase-based technique used to localize tags on a conveyor belt, which takes advantage of the fact that the tagged items move along a conveyor whose path and instantaneous speed are both known. The latter can be implemented with only a firmware upgrade, in any conveyor belt scenario already equipped with an RFID system, without any modification of the system infrastructure and additional (reference tag / multiple antennas) or *ad hoc* hardware. From experimental results in a real scenario, the discrimination between moving tags from static / nomad tags can be obtained with an overall accuracy greater than 99.9%, by employing one reader antenna only.**

***Index Terms*— UHF-RFID systems, phase-based radiolocalization, moving tag, static tag, nomad tag, false positives, stray reads.**

I. Introduction

IN THE last years, the Radio Frequency Identification (RFID) technology is gaining increasing interest for item level tagging applications in logistics, manufacturing, anti-counterfeiting, access control, airport baggage management [1]-[2]. Specifically, the UHF-RFID systems allow for a remote identification without requiring proximity coupling (as needed for bar code readers and HF RFID tags), with the advantages of a low cost deployment, compact tags and high read rates. A large number of tagged items can be concurrently managed and the service process can be faster. Usually, in supply chains, the goods in transit in the warehouse are detected by a UHF-RFID gate, namely an identification point equipped with a UHF-RFID reader and one or more antennas. Due to the large beam-width of standard reader antennas and the multipath effects typical of a crowded indoor scenario, the tagged items passing through the gate are identified together with other tagged items static in the scenario or moving nearby the gate, and stray reads [3] events may occur. Besides, if nearby portals are installed, the problem of undesired readings of tagged items crossing the side portals (also known as cross readings) has to be managed. Above issues lead to solve a classification problem among tagged items passing through the desired RFID gate (true positives) and all others tagged items (static or moving) in the indoor scenario (false positives). It is apparent that a reliable employment of RFID technology in distribution center processes is strictly related to the solution of above problems [4].

The state-of-the-art of techniques for identifying or controlling stray reads at RFID gates is quite limited. Three-dimensional localization techniques could be employed to solve the problem [5]-[6], but a spatial resolution comparable to the size of the tagged items is a challenging goal. Other solutions suggest the possibility to perform the tag proximity detection with *ad hoc* hardware tags or readers, Tag-to-tag Communication Systems or Sense-a-Tag [7]-[8].

Basic approaches employ data related to the antenna detecting the tag and the number of useful readings in an assigned time window [9]. Beside, Received Signal Strength Indicator (RSSI) data can be employed [4], [10]-[11]. In [4], the authors suggest to use various aggregated attributes based on the low-level reader data (Electronic Product Code, RSSI, timestamp, antenna) to perform a classification algorithm in forklift truck applications, getting an overall accuracy of 95.5%. To improve such a performance, the same authors extended the method by using an advanced reader antenna setup [10]. By employing a portal configuration with two readers and eight antennas at the METRO Group (distribution center of Unna, Germany) an overall accuracy of around 99% is obtained, despite of a higher infrastructure cost. In [11], three gate concepts, which differ in the complexity of the underlying algorithms and hardware requirements, have been investigated to discriminate static and moving tags crossing the gate along a conveyor belt and to correctly assign a tagged item to the card box it belongs to. The more robust solution with respect to the box-to-box distance is the “heuristic classification” approach, which classifies a tag as moving if it is recognized by two reader antennas in the right order. It employs RSSI data combined with information from a light barrier sensor.

Beside amplitude-based methods, some solutions exploiting phase-based techniques exist, since phase data could be profitably employed if enough samples can be measured [12]. Intermec patented a method to discriminate among static and moving tags by analyzing the variations of the backscattering signal phase in forklift truck applications [13]. The reader antenna is placed on the forklift and tagged items within the load are static with respect to it. Consequently, tags all around the scenario exhibit a relative motion with respect to them and they can be discriminated. In [14], Sensormatic patented a method based on the Doppler shift to discriminate moving tags in forklift trucks scenario. In [15], a multiple-channel 2D position measurement system for passive UHF-RFID tag arrays based on phase evaluation has been presented. The system combines multiple front-ends, an off-the-shelf RFID reader and passive EPC Gen 2 UHF-RFID transponders, to localize moving as well as static tags with an inverse synthetic aperture radar approach.

Finally, in [3] all available tag information are jointly employed for tag classification in forklift truck applications. The authors proposed an algorithm based on the absolute mean of the Doppler shift, the standard deviation of phase angle rotation and the RSSI that typically assume low values for static tags (named as lay around tags). Besides, the algorithm exploits information about the reader antenna detecting the tag and the number of available readings. Indeed, static tags are typically detected by only one reader antenna in the scenario and several readings can be collected for them, while moving tags across the gate are usually detected by more reader antennas and only few readings are collected.

It is worth noting that the missing tags issue that can occur during tags inventory is outside the aim of this work. To solve such problem, solutions employing statistical methods with redundant reader sessions [16]-[17], cooperative read-points [18] or novel anti-collision protocols [19]-[20] have been proposed in the open literature.

The authors of this paper recently demonstrated that the phase-based localization technique based on a synthetic-array approach proposed in [21]-[22] (named as SARFID - Synthetic Aperture Radar approach for RFID tag localization) can be employed not only to localize tagged items moving along a conveyor belt equipped with a UHF-RFID gate, but also to discriminate them from all other tagged items that are static in the indoor scenario [23]. Indeed, from the SARFID processing is possible to extract some useful parameters to implement a classification algorithm. SARFID only requires for a software / firmware implementation in any conveyor belt scenario already equipped with a passive UHF-RFID system, without any modification of the system infrastructure or additional / *ad hoc* hardware. Differently from other techniques that are used to solve the above misclassification issue, the approach proposed in [23] does not require multiple antennas.

This paper introduces a new classification algorithm for discriminating tags moving along a conveyor belt from all other tags in the scenario. With respect to preliminary results derived in [23] through a standard *k-Means* classification algorithm, the new method employs the features obtained from the SARFID processing [21]-[22] together with the consideration that the phase-variation history of a static tag should be nearly constant. It allows discriminating moving tags along the conveyor belt not only from static tags but also from randomly moving tags, namely nomad tags, still by employing only one reader antenna. The classification is here performed at the tag level, and it can be applied independently on the number of tags that are in the indoor scenario. The paper is organized as follows. In Section II, the UHF-RFID gate scenario is described together with the SARFID technique, while the discrimination issue and the classification algorithm is illustrated in Section III. Finally, classification performance is shown in Section IV and some conclusions are drawn in Section V.

II. UHF-RFID GATE SCENARIO

A typical UHF-RFID gate scenario, where a reader antenna is mounted at a section of a rectilinear conveyor belt, is depicted in Fig. 1. Depending on the reader antenna radiation pattern, static tagged items nearby the conveyor belt can be detected together with the moving tagged items on it. Furthermore, it may happen that tagged items carried out by an operator or moving on a forklift enter the reader antenna radiation pattern and they are identified together with all other tagged items. The latter typically execute a random path, thus they will be referred as nomad tags in the following. Consequently, to correctly manage goods in transit in the warehouse, a discrimination among moving, static and nomad tags is required. Through the paper, we will refer to tagged item as tag.

During the reader inventory, several phase samples can be collected for each tag. For tags moving along the conveyor belt, the phase of the reflected signal complex envelope varies according to the variation of the relative distance between the reader antenna and the tag itself, and a phase-variation history can be measured at the output of the reader I-Q receiver. By considering a static tag placed close to the conveyor belt, a constant phase-variation history is expected. However, due to several effects such as thermal noise, environmental clutter, multipath phenomena, interference from nearby tags, interference from people moving all around the scenario, such a constant behavior could be deeply perturbed and its discrimination becomes more difficult.

As example, let us consider data acquired in a real indoor scenario at Grosseto Airport [24], where a rectilinear conveyor belt is available for baggage recovery. The measurement setup is shown in Fig. 2. The commercial reader Intermec IF2 [25] has been employed, which is able to measure the phase of the tag backscattered complex signal, with 1 degree precision on a 360 degrees range. The reader antenna has been placed in front of the belt at a distance of r_M=210 cm and the belt runs at a speed v=0.5 m/s. The reader output power, the working frequency and the interrogation repetition time have been set at P_{OUT}=29 dBm, f_0=866.3 MHz, and IRT=50 ms, respectively. Above-mentioned system parameters are employed in all the measured results shown throughout the paper. Experiments have been carried out with two antenna typologies: the CAEN WANTENNAX005 antenna [26], with half-power beamwidths equal to $HPBW_H$=$HPBW_V$=67° and $Gain$=6.5 dBic, and the directive MTI Wireless Edge antenna [27] with $HPBW_H$=62°, $HPBW_V$=30° and $Gain$=11 dBic. Both antennas are circularly polarized. Different

commercial tags have been employed for the experiments: the Alien Squiggle ALN 9640 (Alien Higgs-3 chip with -20 dBm read sensitivity [28]) and the LAB-ID UH331 (Impinj Monza5 chip with -18 dBm read sensitivity [29]). The collected measured phase-variation histories are plotted in Fig. 3, for a moving tag (circle markers) and a static tag (square markers), when the wide beamwidth CAEN antenna is used.

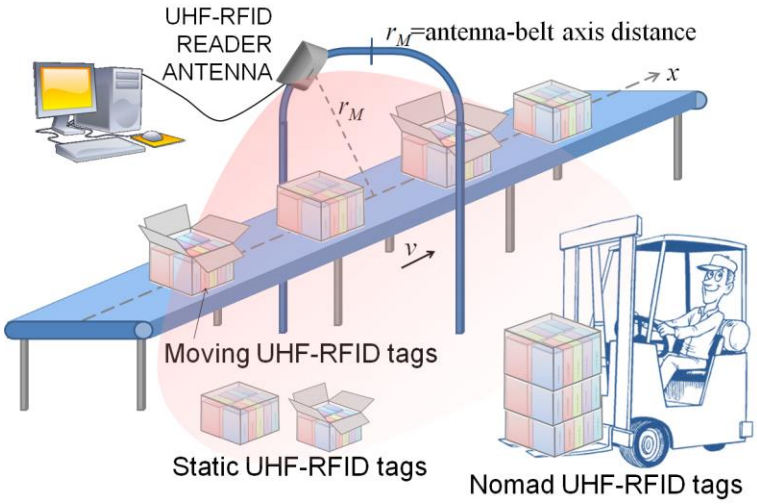

Fig. 1. Conveyor belt geometry with moving tags, static tags and nomad tags in an indoor scenario (v=belt speed, r_M=antenna-belt axis distance).

Fig. 2. Measurement setup at Grosseto Airport to validate the new technique for discriminating moving tags along a conveyor belt from static and nomad tags in a rich multipath environment.

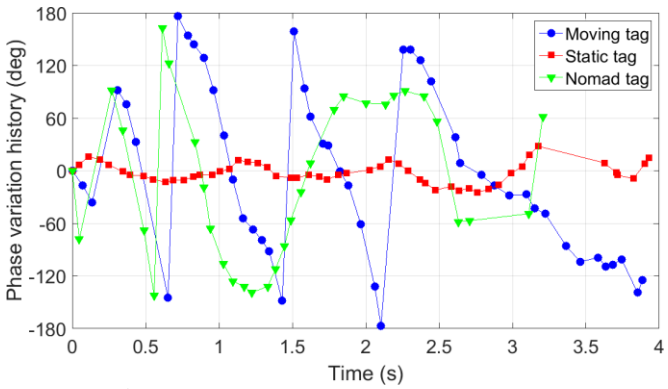

Fig. 3. Measured phase-variation history versus time for a moving tag along a rectilinear conveyor belt (circle markers), a static tag (square marker) and a random tag (triangle marker). N_r={49, 53, 33} readings are collected for each tag, respectively, from the wide beamwidth CAEN antenna.

For each tag, the phase curve is normalized with respect to the phase sample associated to the first available reading. N_r=49 and N_r=53 readings are collected for the moving and the static tags, respectively, in an observation interval of T≈4 s. As expected [21]-[22], an almost quadratic-like phase behavior is observed for the moving tag. In addition, a non-constant curve is got for the

static tag, with a nearby 60° variation range. Fig. 3 also shows the measured phase-variation history related to a nomad tag carried out by a person walking close to the conveyor belt (triangle markers), for N_r=33 available readings. The curve appears completely random because the person walks with an arbitrary motion that cannot be predicted. All these considerations on the tag phase behavior suggest the possibility to perform a discrimination among moving tags and static / nomad ones.

III. TAG CLASSIFICATION

To solve the classification issue it is necessary to find some useful classification features. In this framework, the authors propose the employment of some information available as an output of the SARFID localization technique [21]-[22], which is here briefly summarized. When a tag is moving along a conveyor belt, the phase variations of the reflected signal complex envelope are related to the variation of the relative distance between reader antenna and tag. The SARFID technique exploits the phase-variation history measured at the output of the reader I-Q receiver, by comparing it with nominal phase variations that can be easily constructed if the scenario geometry is known. Indeed, these latter can be analytically evaluated for a given assumed position of the tag on the conveyor at a given reference time, if reader antenna position, belt path and belt speed are all known. Finally, a phase matching operator is applied to determine the nominal history that best fits the measured phase variation history, resembling a (knowledge-based) synthetic array approach. The position associated to the so selected nominal history is chosen as the more likely position of the tag at the reference time. It is worth noting that, due to the anti-collision algorithms implemented in UHF-RFID protocols and also considering that each backscattered signal contains the tag unique identifier, the parallel processing of multiple tags can be easily implemented, so allowing for a real-time localization. The reader can refer to [22] for more details on the SARFID technique and for localization performance in real scenarios.

A. Classification features

By applying the SARFID technique to the phase-variation histories in Fig. 3, the relevant matching functions versus the hypothetical tag position at the reference time [22] are shown in Fig. 4. A well distinct peak appears for the moving tag (solid line) with a maximum value approaching 0.9. On the other hand, several relative maxima can be observed for both the static tag (dashed line) and the nomad tag (dash-dotted line) with a lower peak value around 0.5. This is because the phase profile of static and nomad tags does not match with the expected behavior of a tag moving along the conveyor belt.

The peak value of the matching function can be fruitfully employed as a first classification feature and it can be written as in [22]:

$$C_{max} = \max \frac{\left| \boldsymbol{a}^{H}(s_0')\boldsymbol{y}_p \right|^2}{\left\| \boldsymbol{a}^{H}(s_0') \right\|^2 \cdot \left\| \boldsymbol{y}_p \right\|^2}, \qquad (1)$$

where $a(s_0')$ is the nominal relative phase history, s_0' is the hypothetical tag position and $\boldsymbol{y_p}$ is the phasor obtained from the measured phase history. It is worth noting that the peak position of the matching function represents the estimated tag position at an assumed reference time only for moving tags. The SARFID technique is not effective to locate static or nomad tags, but it can be employed to discriminate them from the moving tags.

To determine a second useful classification feature, the expected behavior of the phase-variation history for a static tag has to be exploited. Since, the latter should be nearly constant, a second classification feature can be determined by calculating a cross-correlation coefficient in the spatial domain, as result of the comparison between a constant phase history and the measured one:

$$C_1 = \frac{\left| \boldsymbol{b}^{H} \boldsymbol{y}_p \right|^2}{\left\| \boldsymbol{b}^{H} \right\|^2 \cdot \left\| \boldsymbol{y}_p \right\|^2}, \qquad (2)$$

where $\boldsymbol{b}$ corresponds to a unitary steering vector.

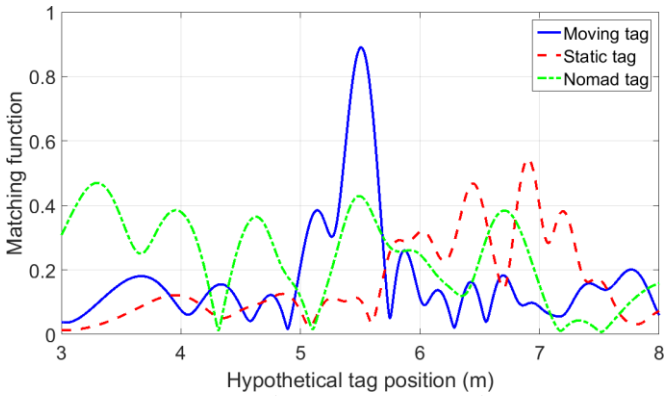

Fig. 4. Matching function versus the hypothetical tag position at the reference time as result of the SARFID processing, for a moving tag along a rectilinear conveyor belt (solid line), a static tag (dashed line) and a nomad tag (dash-dotted line). An observation interval of T=3 s has been employed together with the CAEN antenna.

B. Classification algorithm

Firstly, let us discuss the possibility to discriminate the static tags from the moving ones. To validate the possibility of employing C_{max} and C_1 as classification features, a scatter plot analysis has been carried out. Results are shown in Fig. 5, by considering 5 tags on a box moving along the conveyor belt (circle marker) and 5 static tags nearby the belt (square marker). The CAEN antenna has been employed and results are related to 20 repeated tests.

The measured phase samples have been collected in an observation interval of around T=3 s, which corresponds to a spatial observation interval (namely, the synthetic aperture size [22]) of $D=vT$=150 cm for the tags moving on the conveyor. The circle-point cloud appears well separated from the square-point cloud. Indeed, the C_1 value is lower for the moving tags with respect to the static ones. In particular, as shown in Fig. 6, the ratio C_{max}/C_1 is bigger than one for moving tags, while it is lower than one for static tags. The above ratio differs more and more by increasing the observation interval T of the measured available readings.

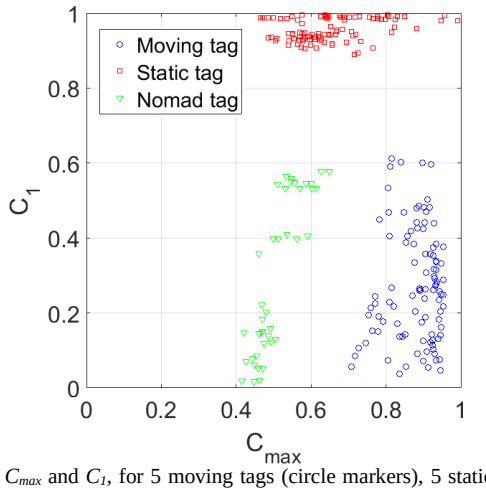

Fig. 5. Scatterplot of the two classification features C_{max} and C_1, for 5 moving tags (circle markers), 5 static tags (square markers) and 2 nomad tags (triangle marker). An observation interval of T=3 s has been employed together with the CAEN antenna.

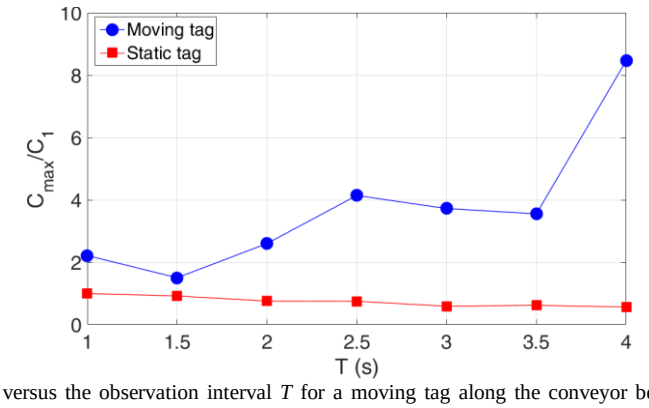

Fig. 6. Classification parameter C_{max}/C_1 versus the observation interval T for a moving tag along the conveyor belt (circle marker) and a static tag (square marker). The CAEN antenna has been employed.

This result confirms the possibility to fruitfully use C_{max} and C_1 as input features of the classification algorithm described in the flow chart of Fig. 7a. It consists of the following steps:

- the phase samples of the tag backscattering signal are collected;
- the SARFID processing is applied to calculate the peak value of the matching function, C_{max};
- the cross-correlation coefficient C_1 is evaluated;
- the ratio C_{max}/C_1 is calculated: if it is greater than 1, the tag is classified as moving, otherwise as static.

Fig. 5 also shows the scatterplot analysis for two nomad tags carried out by a person walking in the scenario (triangle marker). The related point cloud appears separated from the other two, confirming the possibility to discriminate such tag category still employing the above-mentioned features. In particular, a modification of the classification algorithm has been conceived and its flow chart has been represented in Fig. 7b. After the calculation of the ratio C_{max}/C_1 as described in Fig. 7a, a further condition on C_{max} has to be verified: if $C_{max}/C_1>1$ and $C_{max}>\eta$ the tag is classified as moving along the conveyor belt. Otherwise, it is classified as not on the conveyor, being static or nomad. The proper value for the threshold η can be determined empirically.

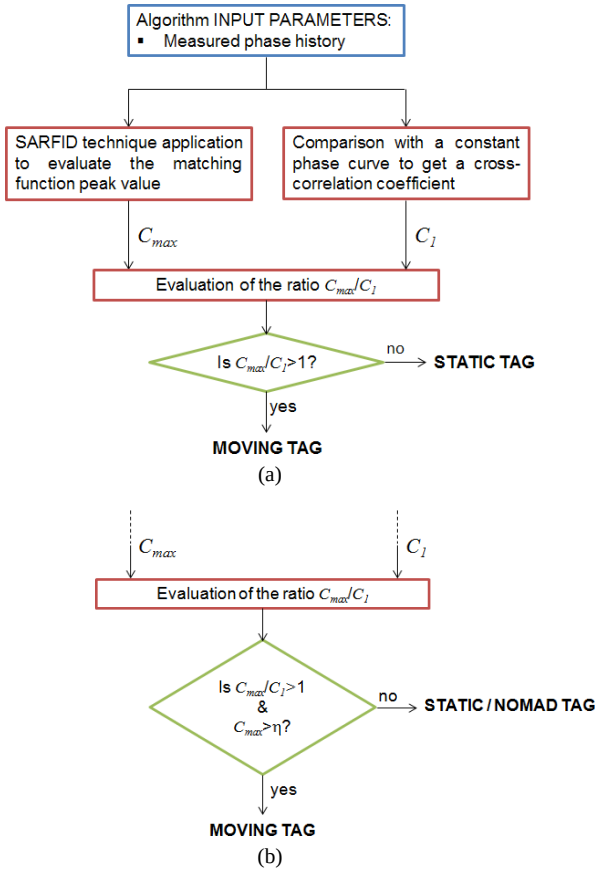

Fig. 7. Flow chart of the classification algorithm employing C_{max} and C_1 to discriminate (a) moving tags along the conveyor belt from static tags and (b) moving tags along the conveyor belt from tags that are not on the conveyor, namely either static or nomad tags.

IV. Classification Performance

A. *Moving tags vs. Static tags*

First experiments have been carried out with 5 tags moving along the conveyor belt at a relative distance of d_{tag}=20 cm, and 5 static tags nearby the belt. To determine the classification performance, repeated tests have been performed. Results have been evaluated through a confusion matrix (Table I), whose row index represents the tag actual class and the column index the tag predicted class [30]. The ratio between the number of correctly classified tags (sum of diagonal terms of the confusion matrix) and the total number of classified tags represents the Overall Accuracy (OA):

$$\text{OA}=\frac{\text{Number of correctly classified tags}}{\text{Total number of classified tags}} \qquad (3)$$

The OA versus the observation interval T, has been represented in Fig. 8a, by considering the two reader antenna typologies: the directive MTI Wireless Edge antenna (circle marker) and the wide beamwidth CAEN antenna (star marker). Each point is the

mean value of 100 test cases. Performance is worse by employing the CAEN antenna with respect to the MTI Wireless Edge antenna. This is meanly due to the wider HPBW in the vertical plane that increases the multipath contribution received together with the line-of-sight signal, and this reduces the percentage of available readings (see as an example Fig.8a and Fig. 9a in [22]). In particular, the read rate reduces from nearby 142 tag/s (MTI Wireless Edge antenna) to 116 tag/s (CAEN antenna). When using the MTI antenna, an overall accuracy greater than 99.9% can be obtained, if the available readings are collected in an interval T>2.5 s that corresponds to a spatial observation interval D>125 cm for moving tags.

	Predicted class	
Actual class	**Moving** tag classified as **moving** tag (True positive)	**Moving** tag classified as **static / nomad** tag (False negative)
	Static / nomad tag classified as **moving** tag (False positive)	**Static / nomad** tag classified as **static / nomad** tag (True negative)

Table I. Confusion matrix to determine the classification performance.

To evaluate the classification algorithm effectiveness, a Receiving Operating Characteristics (ROC) graph has been considered [30]. It consists of the plot of the True Positives Rates (TPR) (4) with respect to the False Positives Rate (FPR) (5):

$$TPR = \frac{\text{Moving tags classified as Moving}}{\text{Number of Moving tags}} \tag{4}$$

$$FPR = \frac{\text{Static/Nomad tags classified as Moving}}{\text{Number of Static/Nomad tags}} \tag{5}$$

The ROC graph is shown in Fig. 8b, when both the directive and wide beamwidth antennas are considered. By increasing the observation interval T, performance approaches the (0, 1) point that represents the perfect classification [30]. In particular, it is reached by employing the MTI Wireless Edge antenna and using an observation interval T>3 s.

Fig. 9a represents the overall accuracy versus the observation interval T, when varying the distance among moving tags, d_{tag}=[15, 20, 25] cm. Each point is the mean value of 150 test cases. By increasing the observation interval, the OA can be improved and it reaches the 99.9% value for phase samples collected for T>2.5 s independently of the moving tag relative distance. The corresponding ROC graph is illustrated in Fig. 9b. Once again, performance improves by increasing the observation interval T.

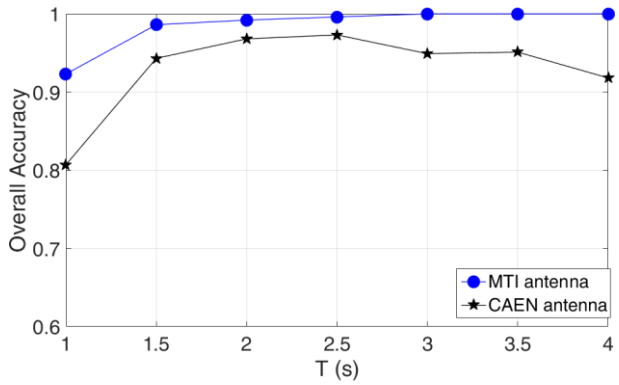

(a)

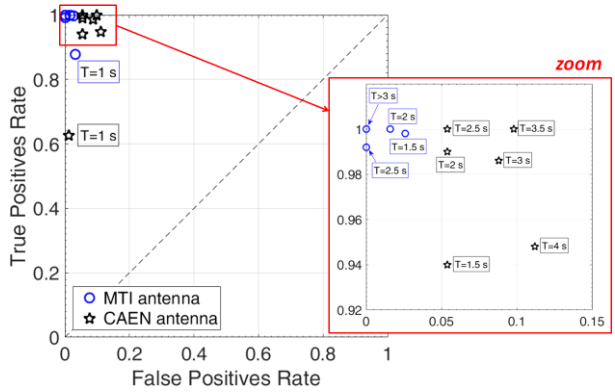

(b)

Fig. 8. (a) Overall Accuracy versus the observation interval T and (b) ROC graph for different observation interval T by varying the reader antenna: MTI Wireless Edge antenna (circle marker) and CAEN antenna (star marker). Each point represents performance of 100 test cases for 5 tags moving along the conveyor belt at a relative distance of d_{tag}=20 cm, and 5 static tags.

B. Moving tags vs. Static / Nomad tags

Now, let us consider the discrimination among moving tags and nomad tags that are present in the indoor scenario together with static tags. Fig. 10 represents the overall accuracy versus the observation interval T, by varying the threshold value η. The distance among the moving tags is d_{tag}=20 cm and the CAEN antenna has been employed. Each point is the mean value of 44 test cases. As expected, classification performance improves by increasing the observation interval T and it is related to the value of the threshold for C_{max}. Best results can be obtained if η=0.6 and T=4 s (D=200 cm for moving tags), as the overall accuracy reaches a value OA=99.9%.

Fig. 11 represents the ROC graph and the number of False Negatives by employing a threshold of η=0.6 for the C_{max} feature. System parameters are as in Fig. 10, still considering 44 test cases. The point (0, 1) of perfect classification is reached for an observation interval of T=4 s. For such value of T, the number of false negatives is equal to zero, which means that moving tags are never missed.

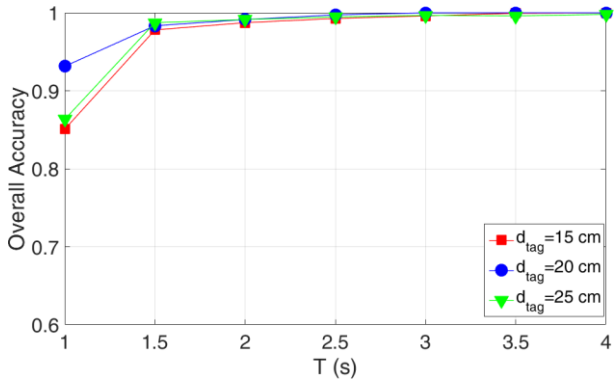

(a)

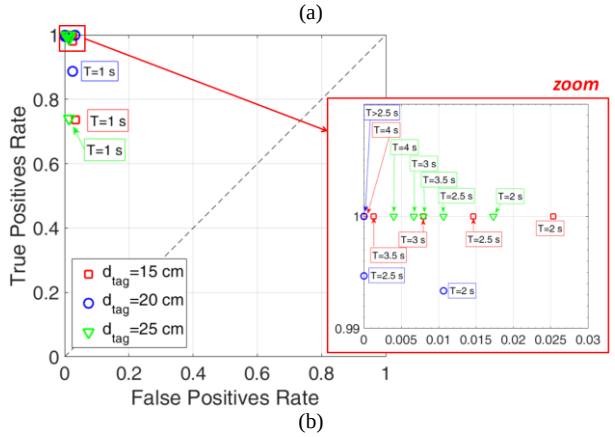

(b)

Fig. 9. (a) Overall Accuracy versus the observation interval T and (b) ROC graph for different values of the observation interval T by varying the relative distance among moving tags: d_{tag}=15 cm (square marker), d_{tag}=20 cm (circle marker) and d_{tag}=25 cm (triangle marker). Each point represents the performance of 150 test cases for 5 tags moving along the conveyor belt and 5 static tags. The MTI Wireless Edge antenna has been employed.

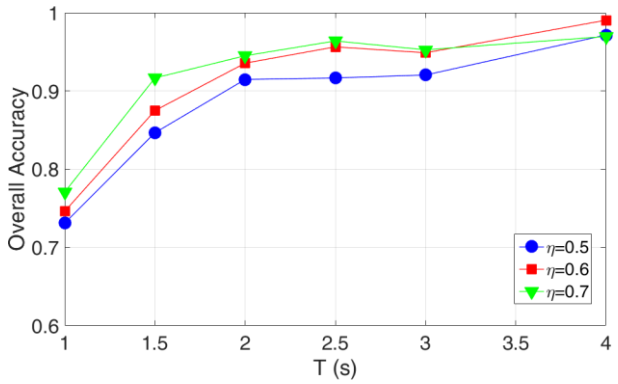

Fig. 10. (a) Overall Accuracy versus the observation interval T by varying the threshold value η for the C_{max} feature. Each point represents the performance of 44 test cases for 5 moving tags along the conveyor belt, 5 static tags and 2 nomad tags. The distance among moving tags is d_{tag}=20 cm and the CAEN antenna has been employed.

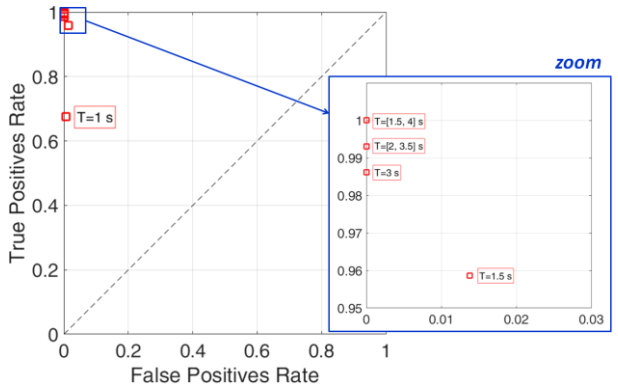

(a)

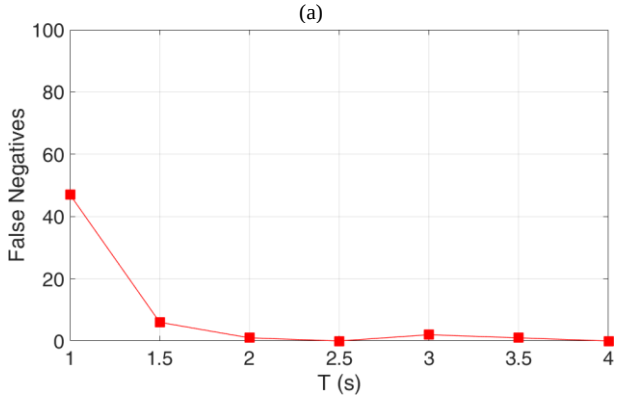

(b)

Fig. 11. (a) ROC graph for different values of the observation interval T and (b) False Negatives versus the observation interval T for 5 moving tags along the conveyor belt, 5 static tags and 2 nomad tags. Each point represents performance of 44 test cases. The threshold η=0.6 has been employed for the C_{max} feature. The distance among moving tags is d_{tag}=20 cm and the CAEN antenna has been employed.

C. Effect of the conveyor belt speed

If the conveyor belt speed increases, the number of available readings for each tag on the conveyor reduces, and the spatial sampling interval of their phase history enlarges. To evaluate such effect, the acquired phase data have been properly managed. In details, if the speed increases of a factor k, the number of available readings reduces of the same factor k and consequently the read rate reduces as illustrated in Table II. Thus, for a constant value of the reader *IRT* parameter (i.e. *IRT*=50 ms), the spatial sampling among readings enhances of the factor k. As illustrated in [22], such spatial sampling has to be less than $\lambda/4$ (≈8.7 cm for f_0=865.7 MHz) to guarantee a satisfactory localization capability of the SARFID technique, and the same condition applies to get good classification performance.

To emulate a conveyor belt moving at speed of v=[1, 1.5, 2] m/s, the phase data acquired for v=0.5 m/s have been under-sampled of a factor k=[2, 3, 4], respectively. Results of the classification performance in terms of Overall Accuracy and ROC graph have been illustrated in Fig. 12. The MTI antenna has been considered with an observation interval of T=3.5 s (circle marker) and T=4 s (cross marker), by using 35 test cases. As shown in Fig. 12a, the OA makes worse when increasing the belt speed. On the ROC graph, the (0, 1) point of perfect classification is still reached for the case of v=1 m/s (Fig. 12b). For v=[1.5, 2] m/s the False Positives Rate keeps equal to zero, but the True Positives Rate is slightly lower than one. These results suggest

that if the conveyor speed increases, the classification algorithm is still able to discriminate tag only if the reader *IRT* parameter is properly reduced to collect phase samples with a spatial sampling rate less than λ/4.

v ***(m/s)***	***Read Rate*** ***(tag/s)***	***Spatial sampling (cm)***
0.5	142	2.5
1	71	5
1.5	35	7.5
2	17	10

Table II. Read rate and spatial sampling by varying the conveyor belt speed *v*, for a reader interrogation repetition time *IRT*=50 ms.

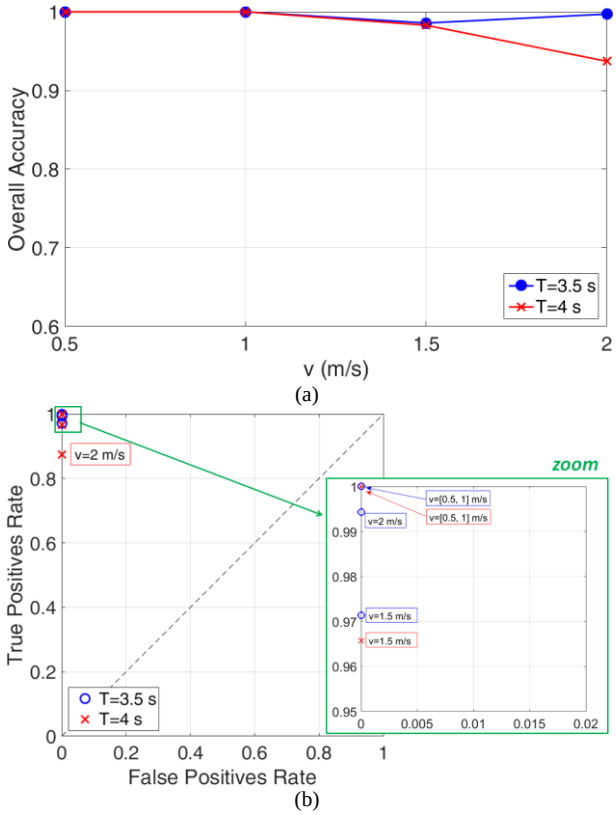

Fig. 12. (a) Overall Accuracy versus the conveyor belt speed *v* and (b) ROC graph for different values of the conveyor belt speed *v*, by varying the observation interval: *T*=3.5 cm (circle marker) and *T*=4 s (cross marker). Each point represents performance of 35 test cases for 5 tagged items at a relative distance of d_{tag}=20 cm moving along the conveyor belt, and 5 static tagged items. The MTI Wireless Edge antenna has been employed.

It is worth noting that, due to the anti-collision algorithms implemented in UHF-RFID protocols and also considering that each backscattered signal contains the tag unique identifier, the classification procedure here proposed can be implemented at single tag level, independently on the tag typology. This is the main difference with respect to a conventional classification algorithm, as for example the *k-Means* algorithm, which is able to perform classification only by considering a group of tags, since it exploits data similarity [23].

For any scenario that does not allow to get an adequate number of phase samples for each detected tag (namely, in case of a low spatial sampling rate) a performance loss is expected [22]. This can happen for high belt speeds, as well as in scenarios with a high tag density, as for example in presence of stacked tags or boxes that are full of small tagged items.

V. Conclusion

A new classification method to discriminate moving tags along a conveyor belt from static and nomad tags in the scenario has been presented. The classification procedure here proposed exploits two classification features. The first one is extracted from the SARFID processing used to localize tags on a conveyor belt. The second classification feature is a cross-correlation coefficient derived by considering that the phase-variation history of a static tag should be nearly constant. A measurement campaign has been carried out at the conveyor belt facility of Grosseto Airport. The discrimination between moving and static tags can be obtained with a 99.9% overall accuracy, if the phase samples are collected in a proper observation interval greater than 2.5 s, independently from the relative distance among nearby tags. By considering also nomad tags, an overall accuracy greater than 99.9% can be obtained for an observation interval *T*=4 s by employing a wide beam reader antenna.

Differently from other methods, the proposed approach can be implemented in any scenario already equipped with a UHF-RFID gate, without additional (e.g. reference tags or multiple antennas) or *ad hoc* hardware. The classification can be performed at the tag level independently from their typology, by using a single reader antenna.

It is worth noting that such classification procedure can be applied in any scenario where tags with a relative motion with respect to the reader antenna have to be discriminated from all other tags, as for example tagged items on a forklift equipped with a reader antenna, or tagged items in warehouses equipped with an overhead travelling crane.

ACKNOWLEDGMENT

The authors thank the "Fondazione Pisa" for the financial support of the research activity, under SARFID project, and the Grosseto Airport administration for allowing the experimental activities within the baggage handling system.

REFERENCES

[1] G. Roussos, "Enabling RFID in retail", *Computer*, vol. 39, no. 3, pp. 25-30, March 2006.

[2] G. M. Gaukler, "Item-Level RFID in a Retail Supply Chain With Stock-Out-Based Substitution", *IEEE Transactions on Industrial Informatics*, vol. 7, no. 2, pp. 362-370, May 2011.

[3] A. S. Toivonen, "Identifying and Controlling Stray Reads at RFID Gates", PhD Thesis, 2012.

[4] T. Keller, F. Thiesse, J. Kungl, E. Fleisch, "Using low-level reader data to detect false-positive RFID tag reads", *2010 Internet of Things* (*IOT*), pp. 1-8, 2010.

[5] S. Shuai and R. J. Burkholder, "Item-level RFID tag location sensing utilizing reader antenna spatial diversity", *IEEE Sensors Journal*, vol. 13, no. 10, pp. 3767–3774, October 2013.

[6] J. Wang and D. Katabi, "Dude, Where's My Card? RFID Positioning That Works with Multipath and Non-Line of Sight", *ACM SIGCOMM Computer Communication Review*, vol. 43, no. 4, pp. 51-62, August 2013.

[7] M. Rostamian, "Localization and proximity detection in the Internet of Things on an Augmented UHF RFID System", Master Thesis, 2014.

[8] M. Bolić, M. Rostamian and P. M. Djurić, "Proximity detection with RFID in the Internet of Things", *48th Asilomar Conference on Signals, Systems and Computers*, Pacific Grove, CA, pp. 711-714, 2014.

[9] Y.-J. Tu and S. Piramuthu, "Reducing False Reads in RFID-Embedded Supply Chains", *Journal of Theoretical and Applied Electronic Commerce Researc*h, vol. 3, no. 2, pp. 60-70, August 2008.

[10] T. Keller, F. Thiesse, A. Ilic, and E. Fleisch, "Decreasing false-positive RFID tag reads by improved portal antenna setups", *2012 3rd International Conference on the Internet of Things (IOT)*, pp. 99-106, October 24-26, 2012.

[11] M. Goller and M. Brandner, "Experimental evaluation of RFID gate concepts", *2011 IEEE International Conference on RFID* (*RFID*), pp. 26-31, April 2011.

[12] J. Huiting, H. Flisijn, A. B. J. Kokkeler, and G. J. M. Smit, "Exploiting phase measurements of EPC Gen2 RFID tags", *2013 IEEE International Conference on RFID Technologies and Applications*, Malaysia, September 4-5, 2013.

[13] S. V. Schatz, G. Spiess, T. Ternes, M. Anderson, and H. Leland, "Utilization of motion and spatial identification in mobile rfid interrogator", US 2009/0207024 A1, Aug. 20, 2009.

[14] G. M. Shafer, "Radio Frequency ID doppler motion detector", US 7,609,163 B2, Oct. 27, 2009.

[15] M. Scherhaufl, M. Pichler, and A. Stelzer, "Localization of Passive UHF RFID Tags Based on Inverse Synthetic Apertures", *2014 IEEE International Conference on RFID*, pp. 82-88.

[16] P. Popovski, K. Fyhn, R. M. Jacobsen, and T. Larsen, "Robust statistical methods for detection of missing RFID tags", *IEEE Wireless Communications*, vol. 18, no. 4, pp. 74-80, August 2011.

[17] K. Fyhn, R. M. Jacobsen, P. Popovski, and T. Larsen, "Fast Capture-Recapture Approach for Mitigating the Problem of Missing RFID Tags", *IEEE Transactions on Mobile Computing*, vol. 11, no. 3, pp. 518-528, March 2012.

[18] M Goller, M Brandner, and G. Brasseur, "A System Model for Cooperative RFID Readpoints", *IEEE Transactions on Instrumentation and Measurement*, vol. 63, no. 10, pp. 2480-2487, October 2014.

[19] C. Shao, T. Kim, J. Yu, J. Choi, and W. Lee, "ProTaR: Probabilistic Tag Retardation for Missing Tag Identification in Large-Scale RFID Systems", *IEEE Transactions on Industrial Informatics*, vol. 11, no. 2, pp. 513-522, April 2015.

[20] H. Wu and Y. Zeng, "Passive RFID Tag Anticollision Algorithm for Capture Effect", *IEEE Sensors Journal*, vol. 15, no. 1, pp. 218-226, January 2015.

[21] P. Nepa, F. Lombardini, A. Buffi, "Method for determining the location of a moving RFID tag," EP2533173 (A1), IP: University of Pisa.

[22] A. Buffi, P. Nepa, and F. Lombardini, "A Phase-Based Technique for Localization of UHF-RFID Tags Moving on a Conveyor Belt: Performance Analysis and Test-Case Measurements", *IEEE Sensors Journal*, vol. 15, no. 1, pp. 387-396, January 2015.

[23] A. Buffi and P. Nepa, "A phase-based technique for discriminating tagged items moving through a UHF-RFID gate", *2014 IEEE RFID Technology and Applications Conference* (*RFID-TA*), pp. 155-158, September 8-9, 2014.

[24] https://grossetoairport.com/

[25] http://www.intermec.com/products/rfidif2a/

[26] http://www.caenrfid.it/en/CaenProd.jsp?mypage=3&parent=107&idmod=761

[27] http://www.mtiwe.com/?CategoryID=278&ArticleID=291

[28] http://www.alientechnology.com/wp-content/uploads/Alien-Technology-Higgs-3-ALN-9640-Squiggle.pdf

[29] http://www.lab-id.com/datasheet/inlay_UHF/UH331.pdf

[30] T. Fawcett, "An Introduction to ROC Analysis", *Pattern Recognition Letters*, vol. 27, no. 8, pp. 861-874.

Alice Buffi (M'10) received the bachelor and master (summa cum laude) degrees in Telecommunications Engineering from the University of Pisa, Pisa, Italy, in 2006 and 2008, respectively. During the under-graduate course, she attempted additional classes to get the final certification of bachelor and master degrees with the *Percorso di Eccellenza Award*. She received the Ph.D. degree in *Applied Electromagnetism in electrical and biomedical engineering, electronics, smart sensors, nanotechnologies* from the University of Pisa in 2012 with *Doctor Europaeus* label. She is currently a Post-Doctoral Researcher with the Department of Information Engineering, University of Pisa. Her research interests include the analysis and design of near-field focused planar microstrip arrays, microstrip antennas design, and near-field coupling analysis in UHF-radio frequency identification (RFID) systems and wireless power transfer. She was a Visiting Ph.D. Student with the Queen Mary University of London, London, U.K., in 2012. Her current research topics are on antenna design for UHF-RFID readers, and new localization / classification techniques for RFID-based smart shelves, gates and conveyor belts. Dr. Buffi was a recipient of the Young Scientist Award from the International Union of Radio Science, Commission B, in 2013 and 2016.

Paolo Nepa received the Laurea (Doctor) degree in electronics engineering (summa cum laude) from the University of Pisa, Italy, in 1990. Since 1990, he has been with the Department of Information Engineering, University of Pisa, where he is currently an Associate Professor. He co-authored more than 80 international journal papers, and more than 150 international conference contributions; he also coauthored 3 chapters in international books and one European patent. In 1998, P. Nepa was at the ElectroScience Laboratory (ESL), The Ohio State University (OSU), Columbus, OH, as a Visiting Scholar supported by a grant of the Italian National Research Council (CNR). At the ESL he was involved in research on efficient hybrid techniques for the analysis of large antenna arrays. His main research interest is in the design of wideband and multiband antennas, mainly for base stations and mobile terminals of communication systems, as well as in the design of antennas optimized for near-field coupling and focusing. More recently, he is involved in channel characterization, wearable antenna design, and diversity scheme implementation, for body-centric communication systems. In the context of RFID systems, he is working on techniques and algorithms for UHF-tag localization and RFID-based smart shelves. He has been a member of the local organizing committee of the 2004 URSI EMTS, Pisa, Italy. He is a member of the Technical Advisory Board of URSI Commission B – Fields and Waves and serves as Associate Editor for the IEEE Antennas and Wireless Propagation Letter. Dr. Nepa received the Young Scientist Award from the International Union of Radio Science, Commission B, in 1998.